

*Full Paper***Bone Morphogenetic Protein-2 (BMP-2) and Vascular Endothelial Growth Factor (VEGF) Transfection to Human Periosteal Cells Enhances Osteoblast Differentiation and Bone Formation**

Mayurach Samee^{1,*}, Shohei Kasugai¹, Hisatomo Kondo¹, Keiichi Ohya², Hitoyata Shimokawa², and Shinji Kuroda¹

¹Section of Oral Implantology and Regenerative Dental Medicine, Department of Masticatory Function Rehabilitation,

²Section of Pharmacology, Department of Hard Tissue Engineering,

Tokyo Medical and Dental University, 1-5-45 Yushima, Bunkyo-ku, Tokyo 113-8549, Japan

Received February 13, 2008; Accepted June 16, 2008

Abstract. Periosteum has been demonstrated to contain mesenchymal progenitor cells differentiating to osteoblasts, and both bone morphogenetic protein-2 (BMP-2) and vascular endothelial growth factor (VEGF) may play important roles in cell-based approaches to bone regeneration. The purpose of this study was to evaluate the feasibility and efficacy of BMP-2 and/or VEGF on periosteal cell differentiation to osteoblasts in vitro and ectopic bone formation in vivo. Human periosteum-derived cells were transfected with BMP-2, VEGF, BMP-2 + VEGF, or vehicle as a control by non-viral gene transfer and then cultured and implanted to nude mice intramuscularly. Real-time polymerase chain reaction analysis of the culture revealed that transgenes for BMP-2 and BMP-2 + VEGF induced more mRNA expression of alkaline phosphatase, collagen type I, and osteocalcin than VEGF and vehicle treatments; additionally, alizarin red S staining, alkaline phosphatase staining, and alkaline phosphatase activity were significantly higher in the BMP-2 + VEGF transgene than in the other versions. After implantation, ectopic bone was observed at 4 weeks and greatly increased at 8 weeks in all groups. In particular, the combination of BMP-2 and VEGF formed significantly more bone at 4 weeks, and VEGF transfection resulted in more blood vessels relative to the conditions without VEGF. Thus, VEGF might enhance BMP2-induced bone formation through modulation of angiogenesis.

Keywords: tissue engineering, periosteal cell, bone morphogenetic protein-2 (BMP-2), vascular endothelial growth factor (VEGF), gene transfer

Introduction

Tissue engineering strategies for bone repair concentrate on combining autologous cells with appropriate absorbable materials and signal molecules. The development of models that use various cell sources has led to tests of various methods of bone engineering. Autologous bone grafts are still considered as the gold standard for reconstruction of compromised bones, due to the lack of immunological rejection mechanisms and presence of stem cells and growth factors that have

osteoinductive and osteoconductive properties (1). However, autologous bone grafting poses a variety of problems, including donor site morbidity. The limited amount of available bone suitable for harvesting and grafting must be considered when autologous bone grafts are being considered. Therefore, an alternative approach would be to apply a cell-based strategy, whereby periosteum-derived cells, for instance, could be grown and have potential for tissue-engineered cartilage and bone repair (2–6). Periosteal cells are easily harvested with minimal morbidity. Periosteum is a heterogeneous multi-layered membrane, consisting of an outer fibrous layer and an inner cambium layer. Periosteum has been demonstrated to have mesenchymal progenitor cells in the cambium layer, which are capable

*Corresponding author. mayu.irm@tmd.ac.jp

Published online in J-STAGE on September 6, 2008 (in advance)

doi: 10.1254/jphs.08036FP

of differentiating to osteoblasts to form a mineralized extracellular matrix under appropriate culture conditions (7–12). Previous studies have reported the bone formation potential of periosteal cells combined with appropriate scaffolds (13–20). For repairing critical-size bone defects, periosteal cells have been shown to induce bone formation and bone healing in animal models (13, 21, 22). Vacanti et al. were the first (23) to publish the report of a clinical case using periosteal cells combined with hydrogel (alginate) and a calcium phosphate scaffold (coral) for bone tissue engineering and other researchers subsequently successfully applied periosteal cells to clinical use for maxillofacial reconstruction and tissue recovery in bone defects (24, 25). Although periosteum contains mesenchymal progenitor cells in the cambium layer, it is difficult to isolate either the cambium layer or mesenchymal progenitors precisely. Therefore, periosteum-derived cells would serve as a mixed population of the whole contents of the periosteum, which may cause difficulty in obtaining a large number of stem/progenitor cells in a primary cell culture, and the introduction of osteogenic factors would be advantageous to increase the osteogenic ability of the mixed population. Synergy between bone morphogenetic protein-2 (BMP-2) and vascular endothelial growth factor (VEGF) has been reported, in which there is an intimate relation to bone development and healing that is advantageous for bone regeneration procedures (26–28). They may play important roles in enhancing the efficiency of cell-based approaches to bone regeneration.

Our study was designed to investigate the feasibility of inducing periosteal cell differentiation to osteoblasts with osteogenesis-related factors BMP-2 and VEGF and then evaluate the efficiency of BMP-2 and/or VEGF on periosteal cells in bone formation. The study consisted of both in vitro and in vivo experiments. The in vitro study examined whether the cells isolated from human periosteum were responsive to BMP-2 and/or VEGF stimulation. The in vivo examination explored the hypothesis that isolated human periosteal cells could be successfully engineered by ex vivo gene transfer to deliver BMP-2 and/or VEGF to induce ectopic bone formation in nude mice.

Materials and Methods

Cell isolation and expansion

The present study was approved by the following institutional committees: the committee for animal experiments and the ethics committee for clinical studies. Periosteum tissues (1 cm²) were harvested from the mandibles or maxillas of three patients undergoing dental implant installation surgeries in the Dental

Hospital at Tokyo Medical and Dental University after obtaining informed consent. After the periosteum tissues were rinsed with phosphate-buffered saline (PBS) containing 100 IU/ml penicillin and 100 µg/ml streptomycin (Gibco, Grand Island, NY, USA), the tissues were minced into small pieces and digested by 0.25% collagenase type II (Gibco) at 37°C for 3 h. The isolated cells were centrifuged at 2000 rpm for 5 min; resuspended in Dulbecco's Modified Eagle Medium (DMEM) (Gibco) supplemented with 10% fetal bovine serum (FBS) (Gibco), 100 IU/ml penicillin, and 100 µg/ml streptomycin; plated in 75-cm² flasks; and cultured at 37°C with 5% CO₂ and 95% humidified air. The medium was changed every 2 days. After cells reached 70% confluent, trypsinization was performed with 0.25% trypsin (Gibco) in PBS for 10 min, and then the cells were subcultured until the third passage for the following analyses.

Plasmid preparation

For the in vitro and in vivo experiments, human BMP-2 exon gene, which was originally cloned by Dr. Yutaka Maruoka (29), was ligated to the *Bam*HI restriction enzyme site of pEGFP-N1 (Clontech Laboratories, Inc., Palo Alto, CA, USA) vector as the BMP-2 plasmid (30) and the human VEGF exon region was originally cloned and encoded in the *Eco*RI multicloning site of pcDNA3.1(+) (Invitrogen Corporation, Calsbad, CA, USA) vector as the VEGF plasmid by Dr. Michiko Suzuki. Then the plasmids were transferred into *Escherichia coli* JM109, subcloned, and purified using an EndoFree Plasmid Maxi Kit (Qiagen, Hilden, Germany).

Transient transfection of human periosteal cells

At passage four, periosteal cells were plated at 2×10^5 cells/well in 1 ml of DMEM supplemented with 10% FBS in the twelve wells of a 12-multiwell plate and evenly divided into four groups for each time point designed for the analyses: 1) Control group, vehicle transfection; 2) BMP-2 group, BMP-2 plasmid transfection (1 µg/well); 3) VEGF group, VEGF plasmid transfection (1 µg/well); and 4) Combination group, BMP-2 and VEGF plasmids co-transfection (1:1 µg/well). Transfection of the cells was performed at day 0 using LipofectamineTM 2000 (Invitrogen) reagents according to manufacturer's instructions. After transfection, cells were washed once with PBS and cultured in DMEM containing 10% FBS with 50 µg/ml ascorbic acid, 10 mM β-glycerophosphate, and 10⁻⁷ M dexamethasone. The culture medium was replaced every 2 days. Cell morphologies were monitored under a phase contrast microscope.

VEGF and BMP-2 production

Levels of human VEGF and BMP-2 proteins in the culture media at 12 h and days 1, 3, 7, 10, 14, 21, 28, and 35 were determined by enzyme-linked immunosorbent assay (ELISA) (Quantikine®; R&D Systems, Minneapolis, MN, USA). Each sample medium was processed according to the manufacturer's instructions. The absorbance was measured by a multi-label counter at a wavelength of 405 nm (Wallace 1420 ARVOsx Multi-label counter; Perkin-Elmer, Boston, MA, USA).

DNA amount and alkaline phosphatase activity

Cells were washed with PBS, scraped, lysed by 0.1% Triton X100 (Sigma, St. Louis, MO, USA), and sonicated to destroy cell membranes. After centrifugation at 15,000 rpm for 10 min at 4°C, 100 µl of supernatant sample was extracted from each sample and assayed for alkaline phosphatase (ALP) activity and DNA content measurements. To determine DNA content, 10 µl of the prepared supernatant of each sample was mixed with 200 µl of 2 µg/ml Hoechst 33258 dye in the wells of a 96-well plate and processed with a fluorescent DNA quantitation kit (Bio-Rad Laboratories, Hercules, CA, USA). The samples were then measured with the Wallace 1420 ARVOsx multi-label counter at emission and excitation wavelengths of 365 and 460 nm, respectively. Subsequently, to assess the quantitative and kinetic determination of ALP activity, 20 µl of the supernatant of each sample was added to 100 µl working solution (*p*-nitrophenylphosphate solution) in the wells of another 96-well plate. The reaction was measured with the multi-label counter at a wavelength of 405. Alkaline phosphatase activity was normalized by total DNA amount at each time point.

Alkaline phosphatase-positive cells and nodule formation

At days 7, 14, 21, and 28, a set of the cultured cells was fixed with 10% neutral buffered formalin and washed with deionized water. Alkaline phosphatase-positive cells were stained with 0.6 mg/ml Fast Blue RR Salt and 0.1 mg/ml naphthol AS-MX phosphate alkaline (Sigma). Another set of the cells was fixed in methanol and rinsed with deionized water. The mineralized nodules were stained with 1% alizarin red S (Sigma). The staining results for ALP-positive cells and nodules were captured in digital images for quantitative analyses. The histogram of each picture was derived and exposed in black and white using the Image J image processing program (NIH, Bethesda, MD, USA). Background of the images was subtracted, and the colors of the images were inverted so that dark pixels would become light and vice versa. The histogram represented the total stained area by counting the number of pixels that corresponded

to the black areas covered by the stains within a maximum of 256 units.

RNA isolation and real-time quantitative RT-PCR

Periosteal cells in culture were lysed in TRIzol® solution (Life Technologies, Burlington, ON, Canada) and total RNA was precipitated in isopropanol. First-strand cDNA was reverse-transcribed from total RNA with SuperScript™ II RNase Reverse Transcriptase (Invitrogen, Burlington, ON, Canada). The expression of osteoblast-related genes was determined using the real-time quantitative reverse transcription-polymerase chain reaction (RT-PCR). Amplification primers are listed in Table 1. SYBR Green-based real-time PCR analysis was carried out with the ABI Prism 7300 Sequence Detection System (Applied Biosystems, Foster City, CA, USA). Expression levels of genes examined were normalized by that of glyceraldehyde 3-phosphate dehydrogenase (GAPDH) within the same sample for in vitro data and further divided with the resulting values of the Control

Table 1. Description of the designed primers and probes

Gene	Forward and reverse primers	Fragment length (bp)
hBMP-2	5'-ggcatcctctccacaaaaga 3'-acgtctgaacaatggcatga	225
hVEGF	5'-ggg cct ccg aaa cca tga act 3'-gag aga gat ctg gtt ccc gaa ac	643
hALP	5'-cca cgt ctt caca ttg ggtg 3'-agactgcgcctggttagttgt	196
hColl I	5'-ctgcaagaacagcattgcat 3'-ggcgtgatggcttattgtt	203
hOC	5'-gtgcagagtcagcaaaaggt 3'-tcagccaactgcacagtc	175
mBMP-2	5'-agc aag gac gtc gtg gtg cc 3'-att att tcg gtg ctg gaa act act	306
mVEGF	5'-atctcaagccgtcctgtgt 3'-gcattcacatctgtgtgt	177
mALP	5'-cacgggagggtcctgtacta 3'-ggaggaagggaagaatccag	223
mColl I	5'-ccc aga gtg gaa cag cga tta c 3'-tgt ctt gcc cca ttc att tgt c	233
mOC	5'-tga cct cac aga tcc caa gcc 3'-ata ccg tag atg cgt ttg tag gc	225
hGAPDH	5'-tga acg gga agc tca ctg g 3'-tcc acc acc ctg ttg ctg ta	307
mGAPDH	5'-ccaccagaagactgtggat 3'-cacattggggtaggaacac	173

Table 2. Formula of real-time PCR analysis

Formula for real-time quantitative PCR	
Delta-delta CT formula	$2^{\Delta\Delta Ct}$
Ratio of gene expression of interest	$(2^{\Delta\Delta Ct})_{\text{experiment}} / (2^{\Delta\Delta Ct})_{\text{control}}$

group following the formula in Table 2.

In vivo ectopic bone formation in nude mice

Gene transfection was performed following the *in vitro* protocol. One week after transfection, periosteal cells were trypsinized and suspended in DMEM containing 10% FBS. The cells were counted and concentrated to 2.5×10^6 cells/ml. Porous β -TCP scaffolds (OSferion[®]; Olympus Co., Ltd., Tokyo; coarse granules, approximately 3 mm in diameter and 5 mg in weight, from 100 to 400 μ m in pore size, 75% porosity, 1050°C sintering temperature) were used in this study. The β -TCP scaffolds (5–6 granules, 30 mg) were soaked in 500- μ l cell suspensions in a 24-multi-well plate. They were then placed in a polycarbonate vacuum desiccator. Low pressure (100 mmHg) was then applied for 100 s. Cell/ β -TCP composites were incubated for 24 h at 37°C with 5% CO₂ and 95% humidified air to ensure the adhesion of cells to β -TCP scaffolds.

Forty-eight male athymic nude mice (Balb/c-nu/nu), 10-week-old, were divided into four groups for two time points (n = 6), following the *in vitro* study. Mice were anesthetized with 100 mg/kg ketamine and 5 mg/kg xylazine by intraabdominal injection. An implant, which consisted of five or six granules of a cell/ β -TCP composite, was aseptically placed into a thigh muscle pouch in each of the bilateral hind legs corresponding to the individual groups. The mice were killed at 4 and 8 weeks after implantation. Twelve specimens from each group were retrieved at each time point, and then a half of the specimens were used for a real-time PCR analysis and the other half were subjected for histological analyses, including an immunohistochemical analysis and *in situ* hybridization.

Preparation of tissue sections

The specimens were harvested at 4 and 8 weeks and immediately fixed in 10% neutral formalin buffer solution (Wako, Osaka) for approximately 24 h at 4°C. The specimens were decalcified in 10% ethylenediamine-tetra-acetic acid (EDTA), pH 6.3, for 14 days at 4°C; washed with diethyl pyrocarbonate (DEPC); dehydrated; and embedded in paraffin (melting point, 56°C–58°C). Histological sections, 5 μ m in thickness at 3 different depths (0.5, 1.0, and 2.0 mm), were cut and transferred onto 3-aminopropyltriethoxy silane-coated glass slides. Each section was stained with hematoxylin

and eosin.

Bone morphometry and quantification

Histological section images were acquired through a light microscope (BZ-8000; Keyence, Osaka). Every two images at each position of 0.5, 1.0, and 2.0 mm in depth, for a total of six images per sample, were subjected to measurement. Bone area was quantified by Image J (NIH) software and expressed as the mean \pm standard deviation.

Immunohistochemistry

Sections were immunohistochemically stained with rat anti-mouse CD31 (PECAM-1) monoclonal antibody (BD Biosciences) for detection of endothelial cells. The primary antibodies were titrated (1:50 dilution) and visualized via a three-step staining procedure in combination with biotinylated anti-rat IgG (H + L) (mouse adsorbed) (Vector Laboratories, Inc., Burlingame, CA, USA) as the secondary antibody and streptavidin-HRP (Vector Laboratories, Inc.) together with the DAB Substrate Kit (Zymed, Invitrogen). Immunohistological images of CD31 were acquired through a light microscope (Keyence BZ-8000). Another set of six images, consisting of two images at the three positions per sample, was selected for the quantification. The CD31-positive vessel-like area was measured by Image J (NIH) software. The area of CD31-positive cell structures was calculated and expressed as the mean \pm S.D.

In situ hybridization

RNA probe preparation: RNA probes for human osteocalcin (175-bp) mRNA were prepared by transcribing cDNAs of the appropriate genes inserted into vectors using the following protocol. cDNAs as PCR products were amplified using RT-PCR with their specific oligonucleotide primer sets designed by Primer3 (v. 0.4.0) software (Whitehead Institute for Biomedical Research, Cambridge, MA, USA) (Table 1). In addition, the products were cloned into pCRII[®]-TOPO[®] vectors and amplified in TOP10F' *E. coli*, and the plasmid DNAs were isolated with an EndoFree Plasmid Maxi Kit (Qiagen). Both sense and antisense digoxigenin-11-UTP-labeled single-strand RNA probes were synthesized with SP6/T7 RNA polymerases prepared using a DIG RNA labeling kit (Roche Diagnostics GmbH, Mannheim, Germany).

***In situ* hybridization for the detection of osteocalcin expression:** In each hybridization experiment, two sets of sections from the same sample were hybridized separately with the antisense and sense riboprobes under identical experimental conditions. *In situ* hybridization was performed with commercial *in situ* hybridization

reagents (Nippon Gene, Tokyo). Hybridization was performed for 16 h at 42°C. After DIG-labeled probes were detected with a commercial nucleic acid detection kit (Roche Diagnostics), each section was stained with methyl green and mounted with Mount-Quick™ mounting medium (SPI Supplies and Structure Probe, Inc., West Chester, PA, USA).

Statistical analyses

Statistical analyses were performed by the statistic software package, 14.0 SPSS for Windows (SPSS Inc., Chicago, IL, USA). Data were analyzed with the nonparametric Kruskal-Wallis test, followed by Mann-Whitney tests for two-group comparisons. Data were considered statistically significant when a *P*-value was equal to or less than 0.05. Results are expressed as mean values \pm S.D.

Results

Periosteal cell morphology in all groups showed a fibroblastic spindle shape initially, which gradually changed to a cuboidal shape similar to osteoblastic cells by day 7 and occasional nodule formation over 14 days in this culture system.

Effects of periosteal cell transfection on BMP-2 and VEGF expression

The ELISA assay showed significantly increased BMP-2 production in the BMP-2 and Combination

(BMP-2 and VEGF) groups compared to those in the Control and VEGF groups ($P < 0.05$) (Fig. 1A). The BMP-2 level of the Combination group was the highest at day 3, decreased by day 14, and then remained similar to that of the BMP-2 group from day 14 to day 35. The VEGF and Control groups did not secrete remarkable levels of BMP-2 protein from day 3 through day 35.

The VEGF levels were markedly increased in the VEGF and Combination groups, significantly higher than those in the Control and BMP-2 groups from 12 hours after transfection, and they continued to increase dramatically from days 1 – 10 ($P < 0.05$) (Fig. 1B). After day 10, the VEGF levels dramatically decreased and were maintained at levels similar to that in the Control group after day 21. The Control and BMP-2 groups did not secrete remarkable levels of VEGF.

Alkaline phosphatase-positive cells

As shown in Figure 2A, ALP was expressed in all groups as early as day 7. Alkaline phosphatase-positive cells gradually increased in intensity over time; both the BMP-2 and Combination groups showed higher intensity of the positive cells than the VEGF and Control groups. Quantification of ALP stains demonstrated that the Combination group had significantly more than the other groups at all time points ($P < 0.05$). There was no significant difference between the Control and VEGF groups (Fig. 2B). These results were correlated to the ones in the ALP bioactivity assay demonstrated in Fig. 2E.

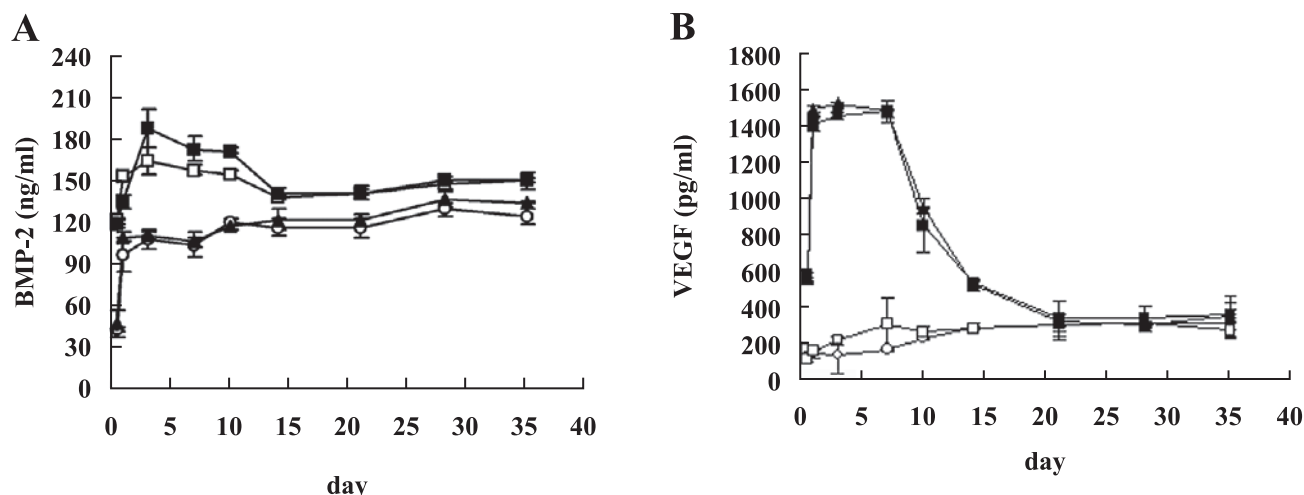


Fig. 1. Protein production in the periosteal cell culture after transfection with BMP-2, VEGF, and a vehicle vector. A: Enzyme-linked immunosorbent assay for BMP-2. The BMP-2 and Combination groups exhibited higher levels of BMP-2 than the VEGF and Control groups over time ($P < 0.05$). B: Enzyme-linked immunosorbent assay for VEGF. The VEGF and Combination groups showed markedly increased VEGF levels at an early time point (12 h) ($P < 0.05$). After 7 days, the VEGF levels in these two groups gradually decreased to levels similar to those in the BMP-2 and Control groups by day 21. Open circle = Control group, open square = BMP-2 group, closed triangle = VEGF group, closed square = Combination group. Values are each expressed as the mean \pm S.D. ($n = 3$). The significance level was set at $P < 0.05$.

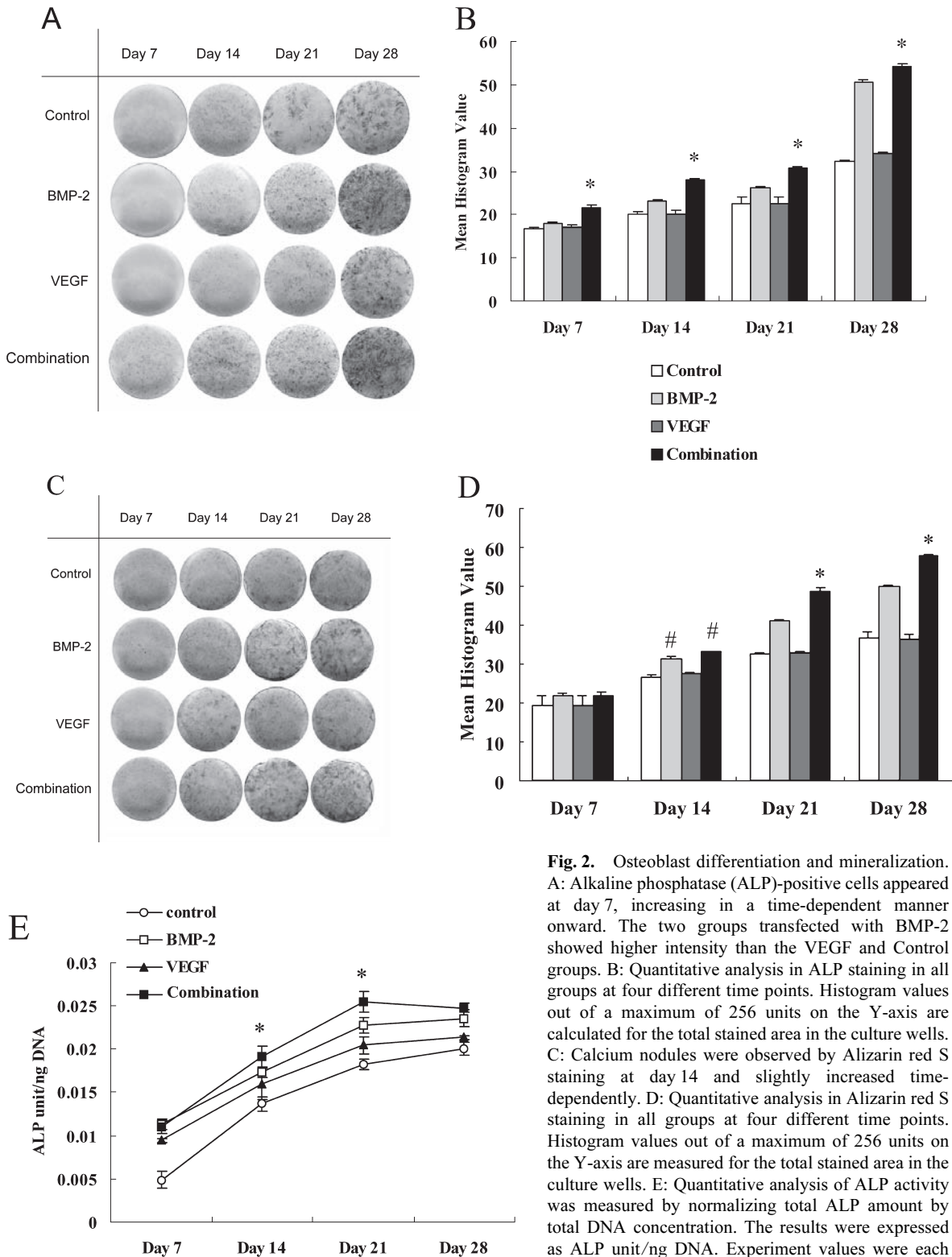


Fig. 2. Osteoblast differentiation and mineralization. A: Alkaline phosphatase (ALP)-positive cells appeared at day 7, increasing in a time-dependent manner onward. The two groups transfected with BMP-2 showed higher intensity than the VEGF and Control groups. B: Quantitative analysis in ALP staining in all groups at four different time points. Histogram values out of a maximum of 256 units on the Y-axis are calculated for the total stained area in the culture wells. C: Calcium nodules were observed by Alizarin red S staining at day 14 and slightly increased time-dependently. D: Quantitative analysis in Alizarin red S staining in all groups at four different time points. Histogram values out of a maximum of 256 units on the Y-axis are measured for the total stained area in the culture wells. E: Quantitative analysis of ALP activity was measured by normalizing total ALP amount by total DNA concentration. The results were expressed as ALP unit/ng DNA. Experiment values were each expressed as the mean \pm S.D. ($n = 3$). *Statistically significant difference compared to all other groups ($P < 0.05$). #Statistically significant difference compared to the Control and VEGF groups ($P < 0.05$).

Effects of BMP-2 and/or VEGF transfection on bone nodule formation

Staining with alizarin red S clearly demonstrated bone nodule formation at day 14; subsequently, a slight increase in the minerals was seen on days 21 and 28 in all groups (Fig. 2C). Quantification of alizarin red S stain showed that there was no significant difference in intensity of the staining among all groups at an earlier time point, day 7. At day 14, the BMP-2 and Combination groups showed no significant difference to each other; however, they exhibited more positive staining than the VEGF and Control groups. Subsequently, the positive staining became significantly higher in the Combination group than in the other groups at days 21 and 28 ($P < 0.05$); however, no significant difference was seen between the Control and VEGF groups over time (Fig. 2D).

Alkaline phosphatase bioactivity

Alkaline phosphatase activity was measured *in vitro* at days 7, 14, 21, and 28. In all groups, ALP activity increased time dependently, but was relatively stable after day 21 (Fig. 2E). All transgene groups showed higher ALP activity than the control over the experimental period. However, the Combination group expressed significantly higher ALP activity than the other transgene groups at days 14 and 21.

In vitro osteoblastic gene expression

As shown in Fig. 3, gene expressions of interest in the cultured cells were evaluated at different time points. In the transgene groups, expressions of ALP, Coll I, and OCN were higher than in the Control group over time. Interestingly, Coll I in the Control group showed very low expression until day 14, but dramatically increased to reach the same level as the transgene groups by day 21. Similarly, the ALP level in the Control group was expressed at a very low level on day 7, but the expression increased significantly to a level similar to those of the transgene groups by day 14. The BMP-2 mRNA level increased in the BMP-2 and Combination groups more than in the Control and VEGF groups. The VEGF mRNA levels in the VEGF and Combination groups were consistently higher than in the Control and BMP-2 groups.

Ectopic bone formation at 4 and 8 weeks

At 4 weeks after implantation, decalcified sections from all groups stained with hematoxylin and eosin exhibited ectopic bone formation in multiple pores of the scaffolds (Fig. 4A). The inner and outer surfaces of the scaffolds were covered with newly formed bone in all groups as early as 4 weeks. The β -TCP scaffold still

remained after 8 weeks. Hematopoietic and fatty marrow-like tissues were also observed in the pore spaces of the scaffolds. Cuboidal cells representing active osteoblasts were observed along the bone-forming surfaces of multiple pore areas, demonstrating active and progressive bone formation, while osteocytic cells appeared embedded in the newly formed bone matrix. By 8 weeks, the amount of bone formed had greatly increased in all groups (Fig. 4A). The result of quantitative analysis of bone formation is shown in Figure 4B. The Combination group had formed the highest amount of ectopic bone at 4 weeks. At 8 weeks, the bone area in the BMP-2 and Combination groups was significantly higher than in the Control and VEGF groups, but there was no significant difference between the BMP-2 and Combination groups. There was also no significant difference between the Control and VEGF groups.

Localization of human osteocalcin mRNA

In situ hybridization was conducted to localize osteoblast-specific gene expression at 4 and 8 weeks after implantation in all groups. Human osteocalcin mRNA expression was observed in cells lining the bone-forming surfaces, indicating the existence of osteoblasts (Fig. 5). The gene expression of human osteocalcin was localized in a similar pattern in all groups. However, hybridization with their sense probes reflected only non-specific signals as normal backgrounds.

Immunostaining for CD31

We analyzed the expression of CD31, a specific marker of endothelial cells, at 4 and 8 weeks. Immunostaining for CD31 revealed angiogenesis occurring at 4 and 8 weeks and capillaries growing into the scaffold (Fig. 6A). Scaffolds without the VEGF transgene showed relatively low blood vessel densities at 4 and 8 weeks. In contrast, the VEGF and Combination groups displayed high densities of blood vessels in the scaffolds. Quantification of blood vessel densities showed that the Combination and VEGF groups had significantly higher blood vessel densities than the BMP-2 and Control groups at 4 and 8 weeks (Fig. 6B).

In vivo osteoblastic gene expressions

Real-time PCR demonstrated mRNA expressions of genes of interest as fold changes to the control level. Human and mouse mRNA expression levels of ALP, Coll I, and OCN were significantly higher in the transgene groups than in the control at two time points (Fig. 7). The levels of expression of ALP, Coll I, and OCN among the groups were ordered as follows: Combination > BMP-2 > VEGF > Control. However, the mVEGF expression level of the BMP-2 group was lower

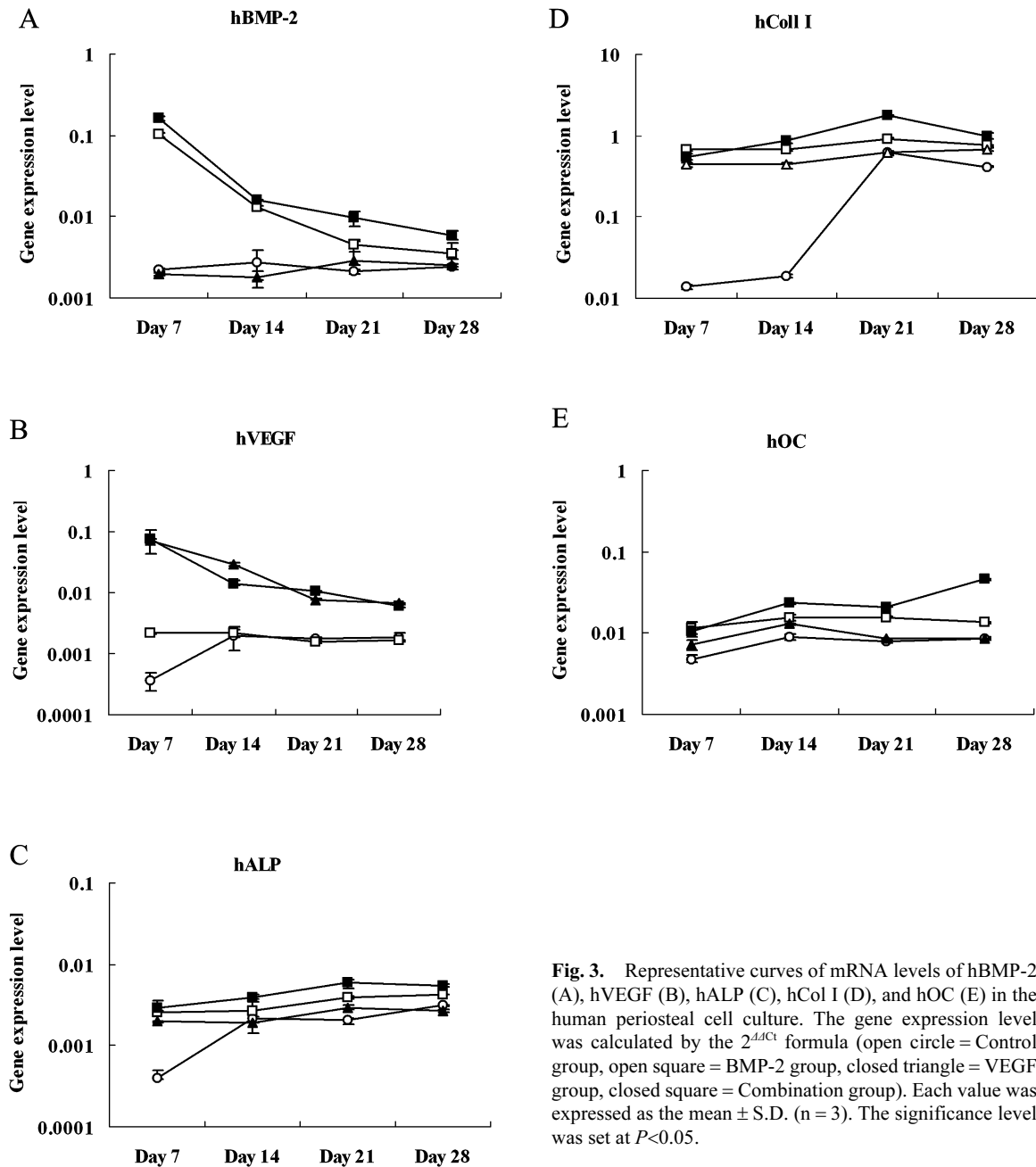


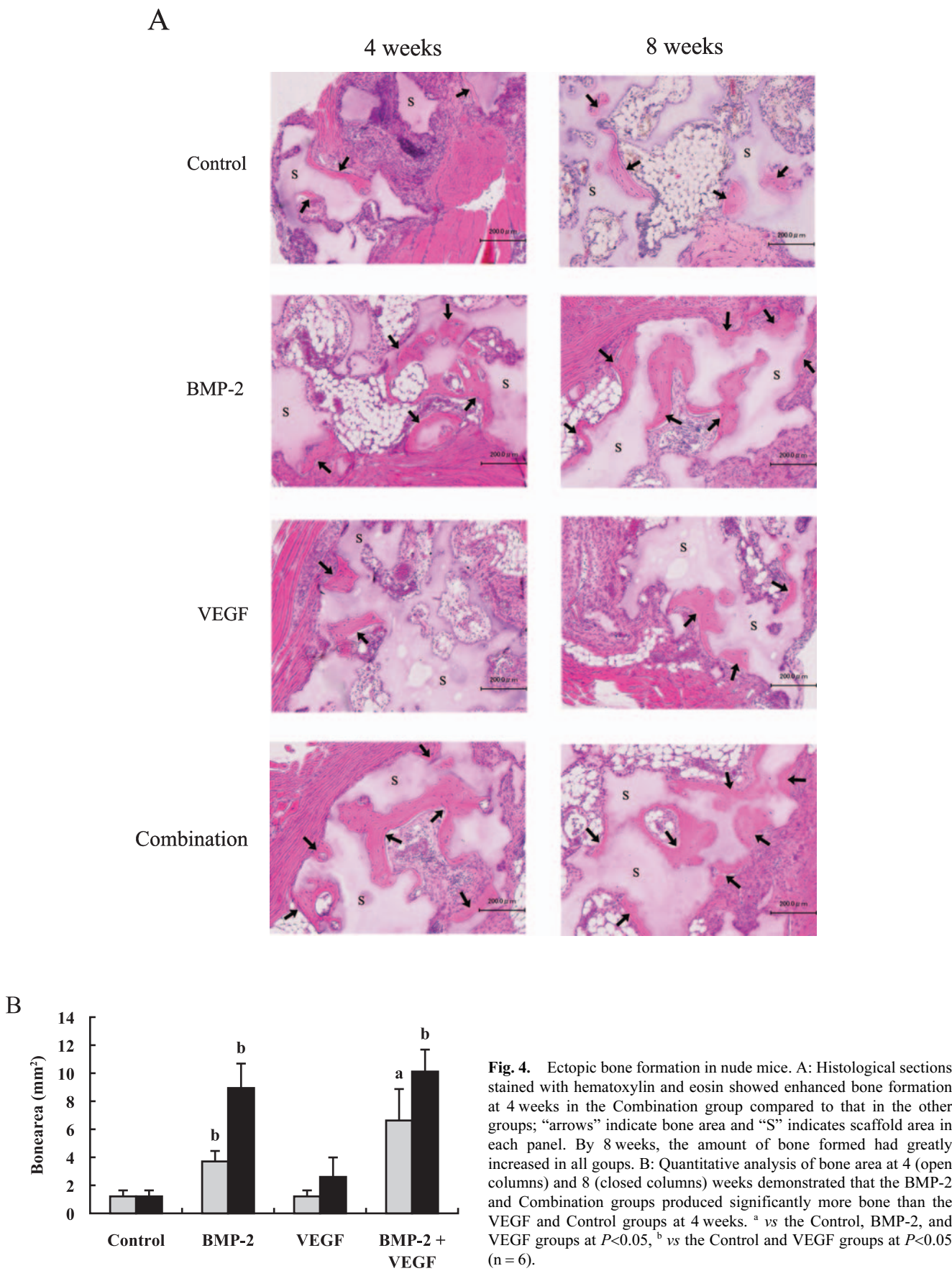
Fig. 3. Representative curves of mRNA levels of hBMP-2 (A), hVEGF (B), hALP (C), hCol I (D), and hOC (E) in the human periosteal cell culture. The gene expression level was calculated by the $2^{-\Delta\Delta C_t}$ formula (open circle = Control group, open square = BMP-2 group, closed triangle = VEGF group, closed square = Combination group). Each value was expressed as the mean \pm S.D. ($n = 3$). The significance level was set at $P < 0.05$.

than in the Control group at 4 weeks. In the VEGF group at 4 weeks, the mRNA levels of hALP, hCol I, mCol I, and mOCN were lower than in the Control group. The BMP-2 expression levels in the BMP-2 and Combination groups were higher than in the Control and VEGF groups. Similarly, the VEGF expression levels in the VEGF and Combination groups were consistently higher than in the Control and BMP-2 groups.

Discussion

Cationic liposome transfection, such as that used in

this study, is a widely used non-viral gene delivery technique, but the efficiency of transfection and toxicity damage to the target cells are still causes for concern. Gene delivery by the lipofectamine reagent is efficient for a wide spectrum of eukaryotic cells; in some cells, the efficiency reaches more than 90% (31, 32). Toxicity to the cells in this technique could be reduced by optimizing the amounts of plasmid and reagents. Indeed, proliferation was not influenced by this transfection but was similar to that under normal conditions without transgenes over the experimental period (data not shown). Therefore, the lipid-mediated DNA delivery



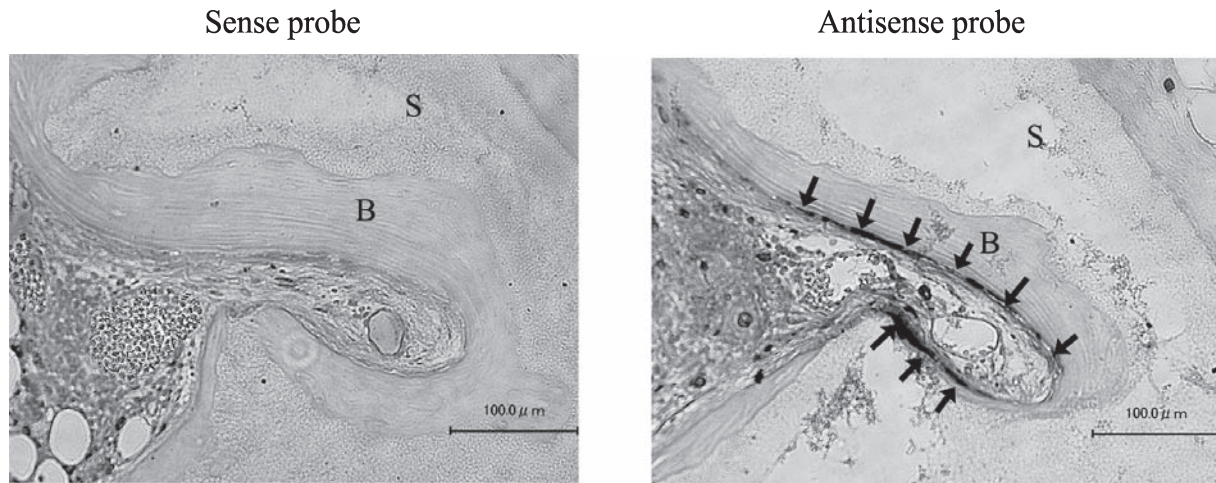


Fig. 5. *In situ* hybridization of the cell/scaffold composite sections using DIG-labeled antisense probes for mRNA of human osteocalcin. A right panel represents mRNA expression of osteocalcin (arrows) localized along the surface of newly formed bone in the Combination group 8 weeks after implantation, implicating the lining of osteoblasts; “B” indicates bone area; and “S” indicates scaffold area.

was considered to be suitable for periosteal cells.

The data indicated that cells transfected with BMP-2 and VEGF could generate higher levels of BMP-2 and VEGF protein expression, respectively. Furthermore, attenuation of BMP-2 and VEGF protein levels was not prominent until day 10; generally, a period of 7 to 14 days is consistent with the early stage of bone formation following osteoblast differentiation. Moreover, BMP-2 protein levels remained higher in the BMP and Combination groups than in the VEGF and Control groups over time. After 7 to 14 days in the BMP-2 and Combination groups, the expression of ALP and Col I was upregulated, suggesting their positive involvement in the process of early osteoblast differentiation. Therefore, the strategy used for gene transfer in this experiment might at least meet an expectation for generating bone.

In this *in vitro* study, periosteal cells could differentiate to osteoblastic lineages, as demonstrated in the present results. Driving periosteal cells with BMP-2 and BMP-2 + VEGF markedly accelerated osteoblast differentiation, as shown in ALP staining and ALP activity. Furthermore, the effect of BMP-2 and VEGF co-transfection was synergistic because the addition of VEGF to BMP-2 showed an increased effect on ALP activity and gene expressions of ALP and OCN (day 28). Moreover, the result of *in vitro* gene expression demonstrated that the gene transfection of BMP-2 and/or VEGF accelerated the early stage of osteoblast differentiation.

It is of interest to note that the expression levels of both ALP and Col I were lower in the Control group, compared to those in the BMP-2, VEGF, and Combina-

tion groups, suggesting that VEGF alone might have an indirect effect on osteoblast differentiation and bone formation. In the ELISA analysis, BMP-2 production was not enhanced in the VEGF group at any time point. Similarly, VEGF production was not stimulated by the BMP-2 transgene alone. These results suggest that the inductions of these proteins did not intimately respond to each other in this culture condition.

It has been reported that cultured periosteal cells formed bone and also cartilage when injected subcutaneously into nude mice (33); However, another study did not obtain such results (34). In the present study, ectopic bone formation was observed using periosteal cells carried in β -TCP scaffolds with transgenes for BMP-2 and/or VEGF. In addition, the combination of BMP-2 + VEGF genes yielded significantly more bone than BMP-2 transfection alone at 4 weeks. Thus, signaling by VEGF transfection could have resulted in more rapid bone formation in the Combination group. Although there was no significant difference between the BMP-2 and Combination groups in bone formation at 8 weeks, a possible explanation for this finding is attributed to the attenuation of the released proteins that were induced by the transgene. Therefore, the accelerating bone formation by BMP-2 and VEGF was observed only at 4 weeks.

Bone formation requires coordination of endothelial cells and osteoblasts, mediated by multiple growth factors and cytokines; BMP-2 and VEGF are two important factors involved in this process (35). The combination of BMP-2 and VEGF has demonstrated enhancement of *in vivo* bone formation through angiogenesis by muscle-derived stem cells transfected with BMP-2 and

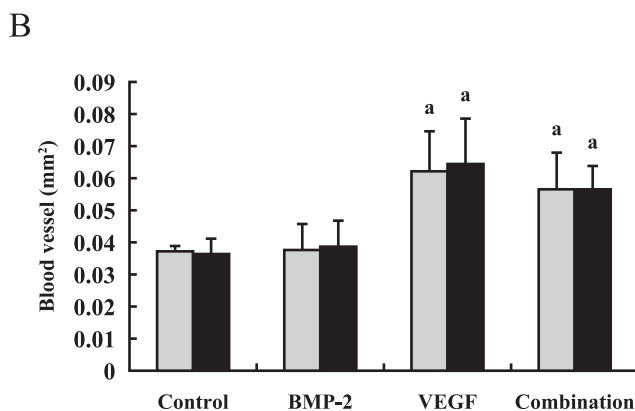
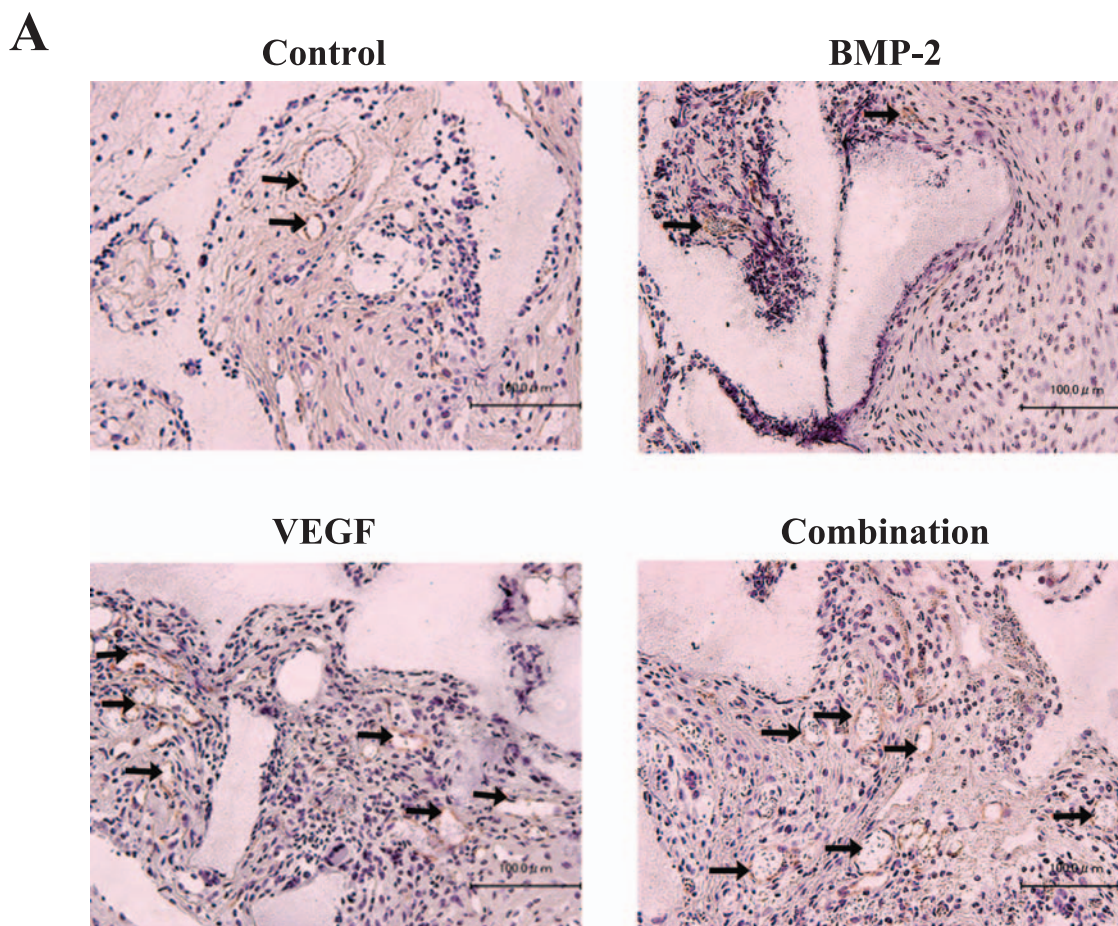


Fig. 6. Immunohistochemistry of CD31 at 4 and 8 weeks. A: Arrows indicate CD31-positive staining (brown), which was indicative of the presence of blood vessels at 4 weeks. The scaffolds containing VEGF transfected cells (VEGF and Combination groups) enhanced blood vessel in growth compared to those with no VEGF transfection (BMP-2 and Control groups). B: Quantitative analysis of blood vessel density within the scaffolds at 4 (open columns) and 8 (closed columns) weeks. The VEGF and Combination groups had significantly higher blood vessel densities than the BMP2 and Control groups throughout the experimental period. ^a vs the BMP-2 and Control groups at $P < 0.05$ ($n = 6$).

VEGF genes (36). The reason for the synergistic or additive effect of BMPs and VEGF on bone formation is still being explored, and there are several possible explanations concerning the role of VEGF: 1) induction of angiogenesis, 2) acceleration of recruitment of host stem cells, and 3) enhancement of cell survival. In our study, transfection with VEGF gene alone was not sufficient to enhance the ability of periosteal cells in bone regeneration compared to the control cells. Similarly, VEGF carried as an adenovirus to muscle-

derived stem cells could not produce ectopic bone in vivo (37). However, in the present in vitro study, gene expressions, protein level, and mineralization were elevated in VEGF-transfected cells, assuming that VEGF has an osteogenic potency.

To identify newly formed bone induced by the exogenous cells, we used β -TCP scaffolds as a carrier because Matsushita et al. in 2004 revealed that no bone formation was observed 6 weeks after intramuscular implantation of β -TCP scaffolds into mice (38). There-

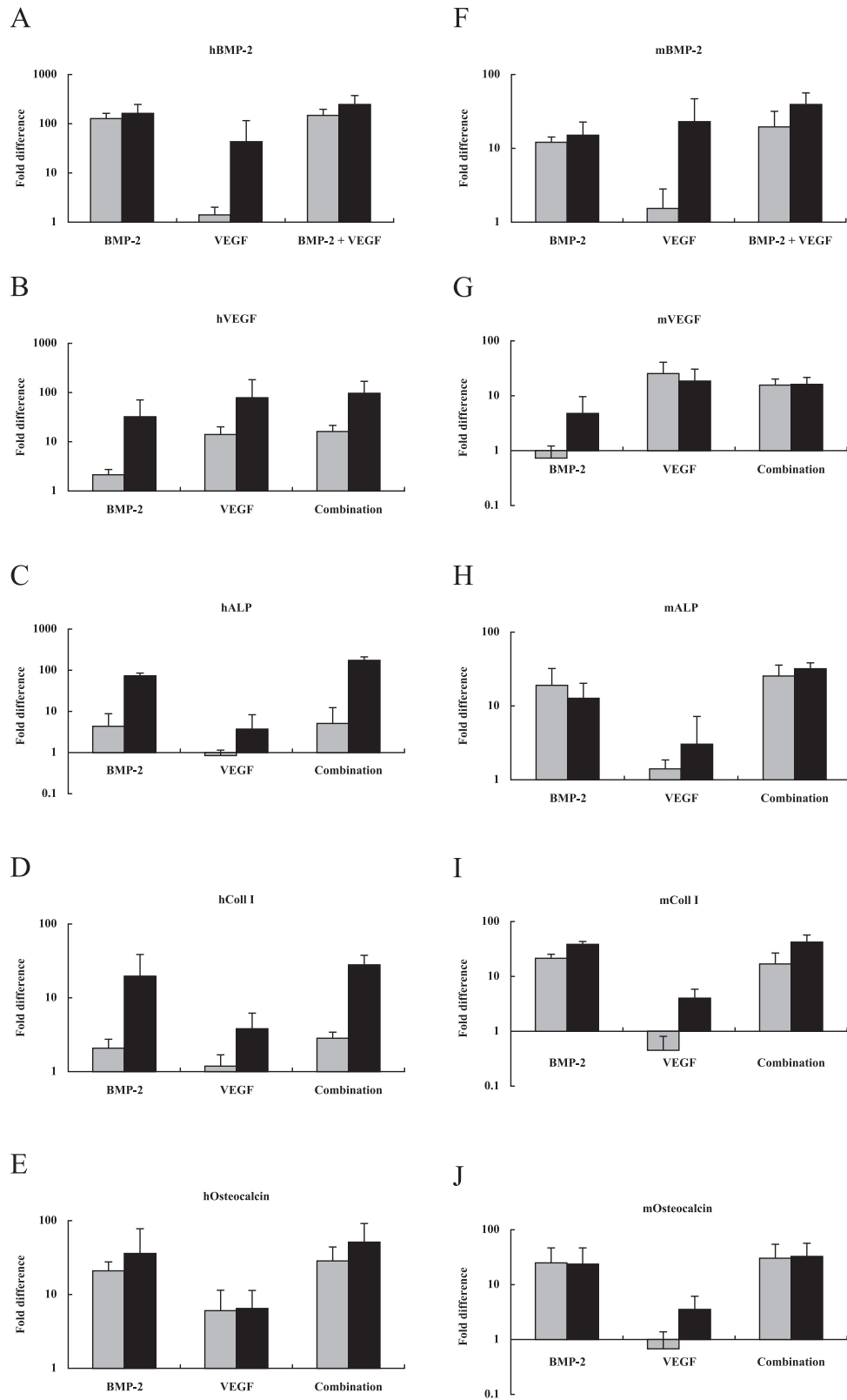


Fig. 7. Messenger RNA expression measured at 4 (open columns) and 8 (closed columns) weeks after implantation. The mRNA levels of hBMP-2 (A), hVEGF (B), hALP (C), hColl I (D), hOC (E), mBMP-2 (F), mVEGF (G), mALP (H), mColl I (I), and mOC (J) were measured from total RNA extracted from the cell/scaffold composites. Messenger RNA expression levels are expressed as fold difference of value in the transgene groups relative to the value in the Control group. Values are each expressed as the mean \pm S.D. ($n = 6$). The significance level was set at $P < 0.05$.

fore, this finding confirms that the ectopic bone formed in our present study can be attributed to the effects of the periosteal cells or the gene-transfected periosteal cells carried with β -TCP scaffolds. Furthermore, although the exogenous cells or host cells were responsible for bone formation, it was difficult to distinguish them by *in situ* hybridization because of the high homology between the nucleotides of the two species. However, the expressions of bone-related genes of mouse and human were observed in RT-PCR analysis, suggesting the involvement of host cells and transplanted cells in ectopic bone formation. The increase of mouse osteoblast-related genes would indicate an influx of adjacent host cells, which differentiated to osteoblasts by the effects of the exogenous human genes.

For successful cell-based bone regeneration, the use of an autologous cell source for cell transplantation is essential and bone marrow mesenchymal stem cells are the most common candidate for bone tissue engineering. Compared to bone marrow cells, periosteal cells can be easily obtained from patients with less invasion and be manipulated as well for autologous transplantation; furthermore, their potential to induce mineralized tissues is not significantly affected by donor age, whereas the number of progenitors in bone marrow declines with age (13, 16, 39–42).

The application of recombinant proteins such as BMPs is considered to be safe for use in humans; however, a large amount of recombinant proteins is necessary to induce sufficient tissue engineering, which becomes costly. In addition, recombinant proteins are unstable and have a short viability, and their localized concentration is difficult to maintain for a certain period *in vivo* (1, 43). Transplantation of the cells carrying genes of these proteins would solve these problems.

Generally, co-transfection may affect expression of concomitant genes and there must be some positive or negative interaction in not only intracellular events but also extracellular modulation. However, in the present study, only the Combination group was designed for “co-transfection” of BMP-2 and VEGF genes but not the Control, BMP-2, and VEGF groups, which should have been processed with the empty vectors. Therefore, although the effect of the co-transfection of BMP-2 and VEGF was not precisely elucidated to be the simply-summed effect of the combined transfections, more bone was observed in the Combination group at post-operative 4 weeks. Thus, we could imply that there was “synergy” in osteogenesis by the BMP-2 and VEGF gene transfer in the periosteal cells. The increase of angiogenesis prominent in this condition probably accelerated *in vivo* bone formation at the early time point. Therefore, the combination of BMP-2 and VEGF

would be effective in bone regeneration and this strategy could be applied to critical-size bone defects or compromised bones that require sufficient vascularization.

Acknowledgments

We acknowledge the assistance of Dr. Michiko Suzuki, research assistant at the Section of Oral Implantology and Regenerative Dental Medicine, Tokyo Medical and Dental University, Tokyo, Japan, in the preparation of the human VEGF plasmid construct. This research was supported by a grant from the Japan Society for the Promotion of Science (No. #17689059) and a grant from the Center of Excellence Program for Frontier Research on Molecular Destruction and Reconstruction of Tooth and Bone at Tokyo Medical and Dental University.

References

- 1 Franceschi RT. Biological approaches to bone regeneration by gene therapy. *J Dent Res*. 2005;84:1093–1103.
- 2 Nakahara H, Bruder SP, Haynesworth SE, Holecck JJ, Baber MA, Goldberg VM, et al. Bone and cartilage formation in diffusion chambers by subcultured cells derived from the periosteum. *Bone*. 1990;11:181–188.
- 3 Nakahara H, Goldberg VM, Caplan AI. Culture-expanded human periosteal-derived cells exhibit osteochondral potential *in vivo*. *J Orthop Res*. 1991;9:465–476.
- 4 Akiyama M, Nonomura H, Kamil SH, Ignatz RA. Periosteal cell pellet culture system: a new technique for bone engineering. *Cell Transplant*. 2006;15:521–532.
- 5 Hutmacher DW, Sittertinger M. Periosteal cells in bone tissue engineering. *Tissue Eng*. 2003;9 Suppl 1:S45–S64.
- 6 Sakata Y, Ueno T, Kagawa T, Kanou M, Fujii T, Yamachika E, et al. Osteogenic potential of cultured human periosteum-derived cells – a pilot study of human cell transplantation into a rat calvarial defect model. *J Craniomaxillofac Surg*. 2006;34:461–465.
- 7 Fang J, Hall BK. Chondrogenic cell differentiation from membrane bone periosteum. *Anat Embryol (Berl)*. 1997;196:349–362.
- 8 Ito Y, Fitzsimmons JS, Sanyal A, Mello MA, Mukherjee N, O'Driscoll SW. Localization of chondrocyte precursors in periosteum. *Osteoarthritis Cartilage*. 2001;9:215–223.
- 9 De Bari C, Dell'Accio F, Vanlauwe J, Eyckmans J, Khan IM, Archer CW, et al. Mesenchymal multipotency of adult human periosteal cells demonstrated by single-cell lineage analysis. *Arthritis Rheum*. 2006;54:1209–1221.
- 10 Fell HB. The osteogenic capacity *in vitro* of periosteum and endosteum isolated from the limb skeleton of fowl embryos and young chicks. *J Anat*. 1932;66:157–180.
- 11 Tang XM, Chai BF. Ultrastructural investigation of osteogenic cells. *Chin Med J (Engl)*. 1986;99:950–956.
- 12 Tenenbaum HC, Palangio KG, Holmyard DP, Pritzker KP. An ultrastructural study of osteogenesis in chick periosteum *in vitro*. *Bone*. 1986;7:295–302.

- 13 Breitbart AS, Grande DA, Kessler R, Ryaby JT, Fitzsimmons RJ, Grant RT. Tissue engineered bone repair of calvarial defects using cultured periosteal cells. *Plast Reconstr Surg*. 1998;101:567–574; discussion 575–576.
- 14 Redlich A, Perka C, Schultz O, Spitzer R, Haupl T, Burmester GR, et al. Bone engineering on the basis of periosteal cells cultured in polymer fleeces. *J Mater Sci Mater Med*. 1999;10:767–772.
- 15 Isogai N, Landis WJ, Mori R, Gotoh Y, Gerstenfeld LC, Upton J, et al. Experimental use of fibrin glue to induce site-directed osteogenesis from cultured periosteal cells. *Plast Reconstr Surg*. 2000;105:953–963.
- 16 Jaquiere C, Schaeren S, Farhadi J, Mainil-Varlet P, Kunz C, Zeilhofer HF, et al. In vitro osteogenic differentiation and in vivo bone-forming capacity of human isogenic jaw periosteal cells and bone marrow stromal cells. *Ann Surg*. 2005;242:859–867, discussion 867–868.
- 17 Ono T, Yoshida T, Hoh C, Davies JE, Sakae T, Nagai N. A morphological study on the response between primary periosteum cultures and synthetic hydroxyapatite particles. *Shika Kiso Igakkai Zasshi*. 1990;32:83–86.
- 18 Perka C, Schultz O, Spitzer RS, Lindenhayn K, Burmester GR, Sittinger M. Segmental bone repair by tissue-engineered periosteal cell transplants with bioresorbable fleece and fibrin scaffolds in rabbits. *Biomaterials*. 2000;21:1145–1153.
- 19 Schantz JT, Hutmacher DW, Chim H, Ng KW, Lim TC, Teoh SH. Induction of ectopic bone formation by using human periosteal cells in combination with a novel scaffold technology. *Cell Transplant*. 2002;11:125–138.
- 20 Spitzer RS, Perka C, Lindenhayn K, Zippel H. Matrix engineering for osteogenic differentiation of rabbit periosteal cells using alpha-tricalcium phosphate particles in a three-dimensional fibrin culture. *J Biomed Mater Res*. 2002;59:690–696.
- 21 Groger A, Klaring S, Merten HA, Holste J, Kaps C, Sittinger M. Tissue engineering of bone for mandibular augmentation in immunocompetent minipigs: preliminary study. *Scand J Plast Reconstr Surg Hand Surg*. 2003;37:129–133.
- 22 Puelacher WC, Vacanti JP, Ferraro NF, Schloo B, Vacanti CA. Femoral shaft reconstruction using tissue-engineered growth of bone. *Int J Oral Maxillofac Surg*. 1996;25:223–228.
- 23 Vacanti CA, Bonassar LJ, Vacanti MP, Shufflebarger J. Replacement of an avulsed phalanx with tissue-engineered bone. *N Engl J Med*. 2001;344:1511–1514.
- 24 Schmelzeisen R, Schimming R, Sittinger M. Making bone: implant insertion into tissue-engineered bone for maxillary sinus floor augmentation—a preliminary report. *J Craniomaxillofac Surg*. 2003;31:34–39.
- 25 Yang ZM, Huang FG, Qin TW. [Bio-derived bone transplantation with tissue engineering technique: preliminary clinical trial]. *Zhongguo Xiu Fu Chong Jian Wai Ke Za Zhi*. 2002;16:311–314.
- 26 Deckers MM, van Bezooijen RL, van der Horst G, Hoogendam J, van Der Bent C, Papapoulos SE, et al. Bone morphogenetic proteins stimulate angiogenesis through osteoblast-derived vascular endothelial growth factor A. *Endocrinology*. 2002;143:1545–1553.
- 27 Furumatsu T, Shen ZN, Kawai A, Nishida K, Manabe H, Oohashi T, et al. Vascular endothelial growth factor principally acts as the main angiogenic factor in the early stage of human osteoblastogenesis. *J Biochem (Tokyo)*. 2003;133:633–639.
- 28 Itoh F, Itoh S, Goumans MJ, Valdimarsdottir G, Iso T, Dotto GP, et al. Synergy and antagonism between Notch and BMP receptor signaling pathways in endothelial cells. *Embo J*. 2004;23:541–551.
- 29 Endo M, Kuroda S, Kondo H, Maruoka Y, Ohya K, Kasugai S. Bone regeneration by modified gene-activated matrix: effectiveness in segmental tibial defects in rats. *Tissue Eng*. 2006;12:489–497.
- 30 Maruoka Y, Oida S, Iimura T, Takeda K, Asahina I, Enomoto S, et al. Production of functional human bone morphogenetic protein-2 using a baculovirus/Sf-9 insect cell system. *Biochem Mol Biol Int*. 1995;35:957–963.
- 31 Hawley-Nelson P. Lipofectamine reagent: a new, higher efficiency polycationic liposome transfection reagent. *Focus*. 1993;15:73–79.
- 32 Kim SW, Ogawa T, Tabata Y, Nishimura I. Efficacy and cytotoxicity of cationic-agent-mediated nonviral gene transfer into osteoblasts. *J Biomed Mater Res A*. 2004;71:308–315.
- 33 Nakahara H, Bruder SP, Goldberg VM, Caplan AI. In vivo osteochondrogenic potential of cultured cells derived from the periosteum. *Clin Orthop Relat Res*. 1990;223–232.
- 34 Zhang C. A study on a tissue-engineered bone using rhBMP-2 induced periosteal cells with a porous nano-hydroxyapatite /collagen/poly(L-lactic acid) scaffold. *J Biomed Mater Res*. 2006;1:52–62.
- 35 Raida M, Heymann AC, Gunther C, Niederwieser D. Role of bone morphogenetic protein 2 in the crosstalk between endothelial progenitor cells and mesenchymal stem cells. *Int J Mol Med*. 2006;18:735–739.
- 36 Peng H, Usas A, Olshanski A, Ho AM, Gearhart B, Cooper GM, et al. VEGF improves, whereas sFlt1 inhibits, BMP2-induced bone formation and bone healing through modulation of angiogenesis. *J Bone Miner Res*. 2005;20:2017–2027.
- 37 Peng H, Wright V, Usas A, Gearhart B, Shen HC, Cummins J, et al. Synergistic enhancement of bone formation and healing by stem cell-expressed VEGF and bone morphogenetic protein-4. *J Clin Invest*. 2002;110:751–759.
- 38 Matsushita N, Terai H, Okada T, Nozaki K, Inoue H, Miyamoto S, et al. A new bone-inducing biodegradable porous beta-tricalcium phosphate. *J Biomed Mater Res A*. 2004;70:450–458.
- 39 Ito Y, Tanaka N, Fujimoto Y, Yasunaga Y, Ishida O, Agung M, et al. Bone formation using novel interconnected porous calcium hydroxyapatite ceramic hybridized with cultured marrow stromal stem cells derived from Green rat. *J Biomed Mater Res A*. 2004;69:454–461.
- 40 Koshihara Y, Kawamura M, Endo S, Tsutsumi C, Kodama H, Oda H, et al. Establishment of human osteoblastic cells derived from periosteum in culture. *In Vitro Cell Dev Biol*. 1989;25:37–43.
- 41 Muschler GF, Midura RJ. Connective tissue progenitors: practical concepts for clinical applications. *Clin Orthop Relat Res*. 2002;66–80.
- 42 Muschler GF, Nitto H, Boehm CA, Easley KA. Age- and gender-related changes in the cellularity of human bone marrow and the prevalence of osteoblastic progenitors. *J Orthop Res*. 2001;19:117–125.
- 43 Govender S, Csimma C, Genant HK, Valentin-Opran A, Amit Y, Arbel R, et al. Recombinant human bone morphogenetic protein-2 for treatment of open tibial fractures: a prospective, controlled, randomized study of four hundred and fifty patients. *J Bone Joint Surg Am*. 2002;84-A:2123–2134.